JOC Article

Fine-Tuning of Radiolysis Induced Emission by Variable Substitution of Donor-/Acceptor-Substituted Tetrakis(arylethynyl)benzenes

Shingo Samori, Sachiko Tojo, Mamoru Fujitsuka, Eric L. Spitler,† Michael M. Haley,† and Tetsuro Majima*

The Institute of Scientific and Industrial Research (SANKEN), Osaka University, Mihogaoka 8-1, Ibaraki, Osaka 567-0047, Japan

majima@sanken.osaka-u.ac.jp

Received January 21, 2008

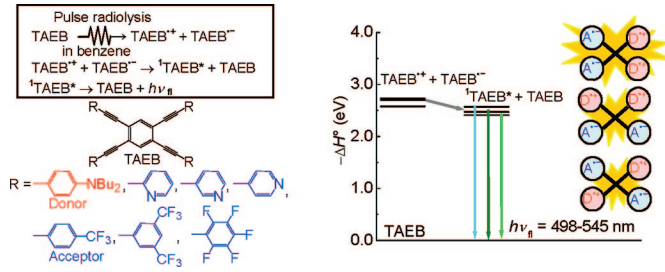

Emission from charge recombination between radical cations and anions of various tetrakis(arylethynyl)benzenes (TAEBs) was measured during pulse radiolysis in benzene (Bz). The formation of TAEB in the excited singlet state (^{1}TAEB*) can be attributed to the charge recombination between TAEB$^{\bullet+}$ and TAEB$^{\bullet-}$, which is initially generated from the radiolytic reaction. It was found that the charge recombination between TAEB$^{\bullet+}$ and TAEB$^{\bullet-}$ gave ^{1}TAEB* as the emissive species but not excimers because of the large repulsion between substituents caused by the rotation around C−C single bonds. Since donor-/acceptor-substituted TAEBs possess three types of charge-transfer pathways (linear-conjugated, cross-conjugated, and "bent"-conjugated pathways between the donor and acceptor substituents through the ethynyl linkage), the emission spectra of ^{1}TAEBs* with intramolecular charge transfer (ICT) character depend on the substitution pattern and the various types of donor and acceptor groups during pulse radiolysis. Through control of the substitution pattern (e.g., the position of the nitrogen atom within the pyridine ring or the number of acceptors per arene ring of the regioisomeric donor-/acceptor-substituted TAEBs with donating *N*,*N*-dibutylamino and accepting pyridine unit (**N1–9**) and those with donating *N*,*N*-dibutylamino and accepting one (**F1–3**), two trifluoromethyl (**F4–6**), or perfluorinated arene (**F7–9**) units), fine-tuning of radiolysis induced emission color can be achieved.

Introduction

Electron detachment from and attachment to a solute molecule (M) generates radical cations (M$^{\bullet+}$) and anions (M$^{\bullet-}$), respectively. M$^{\bullet+}$ and M$^{\bullet-}$ are known as important ionic intermediates in photochemistry, electrochemistry, and radiation chemistry.[1] It is well-known that M in the excited states (M* = ^{1}M* (excited singlet state) and ^{3}M* (excited triplet state)) can be formed by charge recombination between M$^{\bullet+}$ and M$^{\bullet-}$ (M$^{\bullet+}$ + M$^{\bullet-}$ → M* + M), after which ^{1}M* deactivates to M in the ground state by emitting light (^{1}M* → M + $h\nu_{fl}$).[2] This process is significant for optoelectronic materials such as OLEDs because electrochemical energies can be converted to photochemical energies.

Recently, we have found that various 1,2,4,5-tetrakis(arylethynyl)benzenes (TAEBs: namely, 1,2,4,5-tetrakis(phenylethynyl)benzene (TPEB), 1,2,4,5-tetrakis(*N*,*N*-dibutylaminophenyl)benzene (tetra-donor TPEB), and regioisomeric donor-/

† Department of Chemistry and the Materials Science Institute, University of Oregon, Eugene, Oregon 97403-1253.

(1) (a) Fox, M. A.; Chanon, M. *Photoinduced Electron Transfer*; Elsevier: Amsterdam, 1988. (b) Kavarnos, G. J.; Turro, N. J. *Chem. Rev.* **1986**, *86*, 401.

(2) (a) Faulkner, L. R.; Bard, A. J. *Electroanalytical Chemistry*; Marcel Dekker; New York, 1977; Vol. 10, pp 1–95. (b) Bard, A. J.; Faulkner, L. R. *Electrochemical Methods Fundamentals and Applications*, 2nd ed.; John Wiley and Sons: New York, 2001; pp 736−745. (c) Richter, M. M. *Chem. Rev.* **2004**, *104*, 3003.

10.1021/jo8001535 CCC: $40.75 © 2008 American Chemical Society
Published on Web 04/02/2008

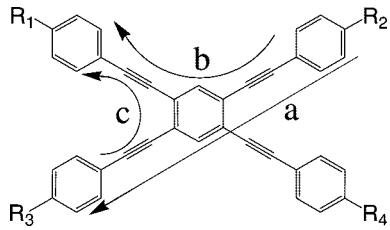

FIGURE 1. Three types of charge-transfer conjugated pathways in TAEBs containing two-donor and two-acceptor functionality shown by arrows.

acceptor-substituted 1,2,4,5-tetrakis(phenylethynyl)benzenes with donating *N*,*N*-dibutylamino and accepting cyano or nitro groups (donor-/acceptor-substituted TPEB)) showed emission during pulse radiolysis in benzene (Bz).[3] In pulse radiolysis of M in Bz, the ionization of Bz to give the Bz radical cation ($Bz^{\cdot+}$) and formation of an electron (e^-) occur at the same time and react with M to give $M^{\cdot+}$ and $M^{\cdot-}$, respectively. In our previous work, we have proposed that the charge recombination of $M^{\cdot+}$ and $M^{\cdot-}$ gives $^1M^*$ and/or $^1M_2^*$ as the emissive species for the organic electrochemiluminescent molecules such as phenylquinolinylethynes,[4a] phenyl(9-acridinyl)ethynes,[4b] phenyl(9-cyanoanthracenyl)ethynes,[4b,d] arylethynylpyrenes,[4c] and 9-cyano-10-(*p*-substituted phenyl)anthracenes.[4e] Consequently, we assumed that the charge recombination between $TAEB^{\cdot+}$ and $TAEB^{\cdot-}$ also results in the formation of $^1TAEB^*$ as the emissive species during pulse radiolysis.

For optoelectronic applications, organic compounds possessing a high degree of π-conjugation with donor and/or acceptor groups have been recognized as ideal materials.[5–7] Changes in the substituents and substitution pattern, electronic structure, and conjugation can provide highly variable photophysical properties for such materials. As a class of π-conjugated molecules with remarkable optoelectronic properties, functionalized cruciform-conjugated phenylacetylene structures have received considerable attention because of their multiple conjugated pathways.[7–9] In particular, the TAEB framework containing two-donor and two-acceptor functionality is an ideal system for studying the differences between the linear-conjugated (Figure 1, path a), cross-conjugated (path b), and "bent"-conjugated (path c) pathways to gain a better understanding of the geometric aspects of the charge-transfer pathways. By varying the substitution pattern of the donor and acceptor groups, each charge-transfer pathway can be modified. Since three different types of charge-transfer conjugated pathways are known for individual donor-/acceptor-substituted TAEBs, we can easily fine-tune the emission wavelength and intensity by changing the substitution pattern and the various types of donor and acceptor substituents. These compounds are also useful for luminescent materials because most of them exhibit sufficient emission efficiency in the region of visible light. In addition, TAEBs can rotate freely about their C−C single bonds,[88] decreasing π-orbital overlap, and thus formation of the face-to-face excimer structure with less luminescence intensity cannot be expected during pulse radiolysis. The time-resolved transient absorption and emission measurements during the pulse radiolysis of various TAEBs are useful to gain a better understanding

SCHEME 1

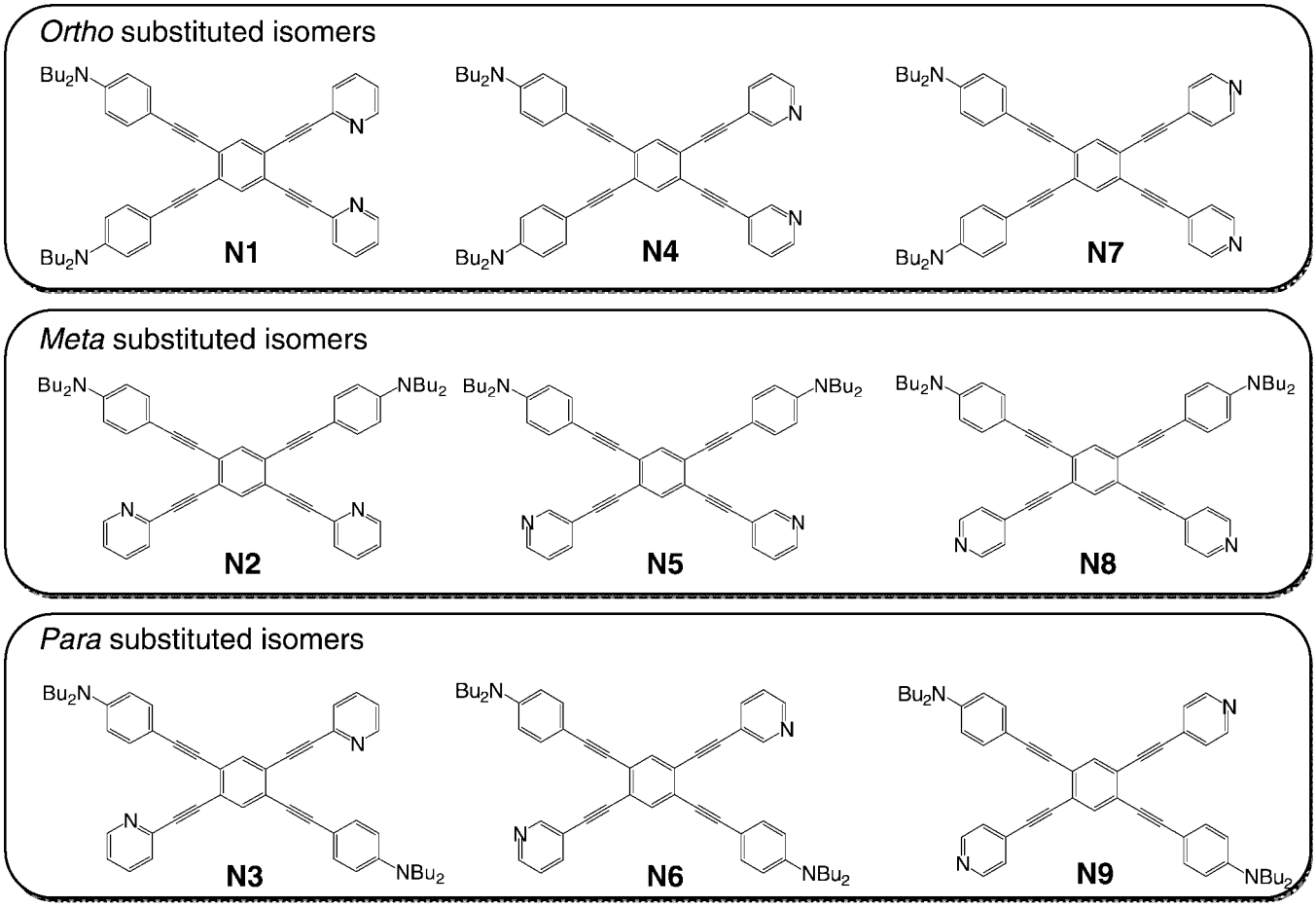

SCHEME 2

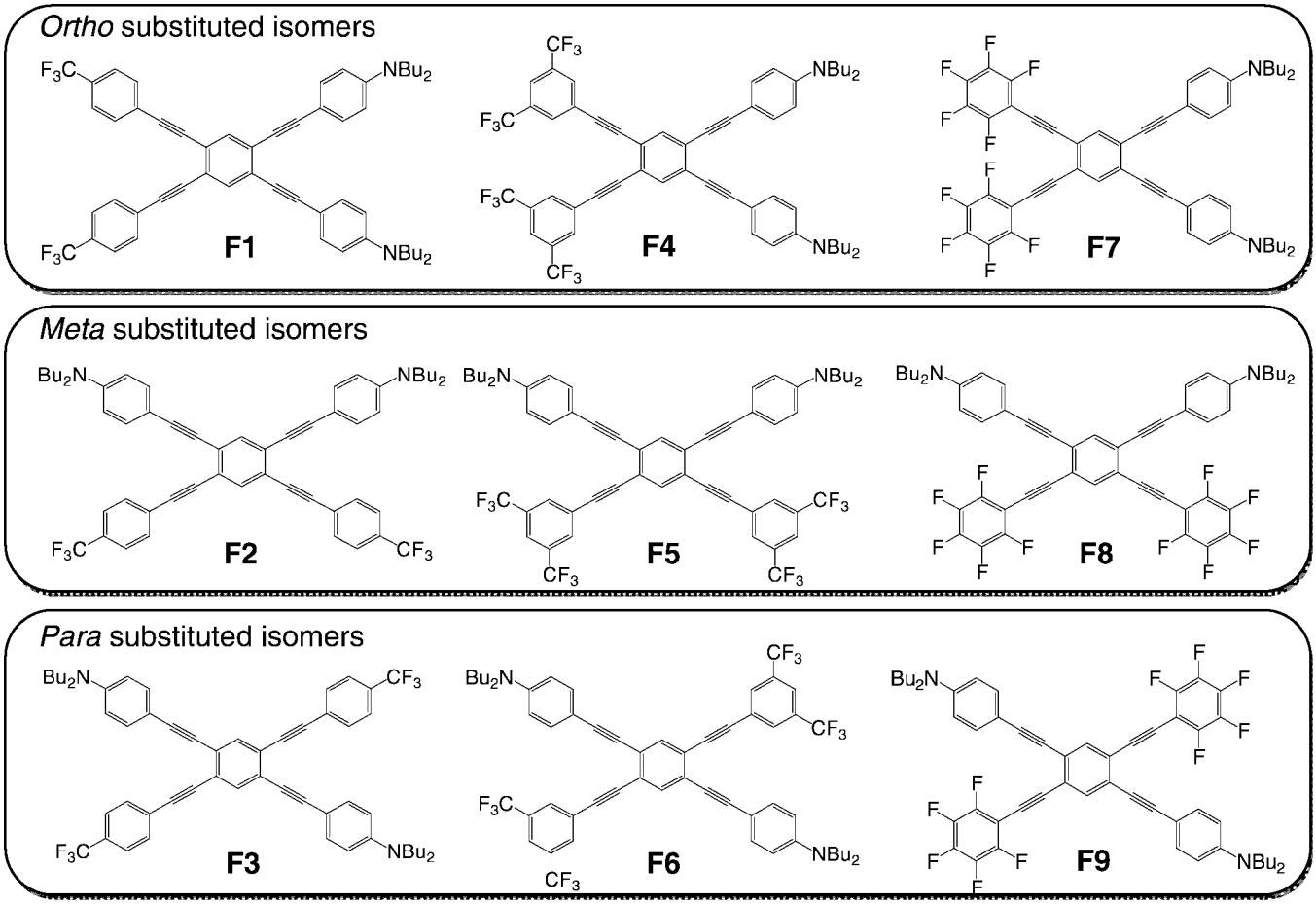

of the emission mechanism, providing valuable information for molecular design with efficient luminescence character.

In this paper, we report the emission from the charge recombination between $TAEB^{\bullet+}$ and $TAEB^{\bullet-}$ of 18 different donor–acceptor tetrakis(arylethynyl)benzenes (TAEBs = **N1**-**9** (Scheme 1) and **F1–9** (Scheme 2)): regioisomeric donor-/acceptor-substituted TAEBs with donating *N*,*N*-dibutylamino and accepting pyridine unit (**N1–9**)[8c] and those with donating *N*,*N*-dibutylamino and accepting one (**F1–3**), two trifluoromethyl (**F4–6**), or perfluorinated arene (**F7–9**) units.[8d]These donor-/acceptor-substituted TAEBs (**N1–9** and **F1–9**) have two donor and two acceptor groups with like substituents fused *ortho* (**N1**, **N4**, **N7**, **F1**, **F4**, and **F7**), *meta* (**N2**, **N5**, **N8**, **F2**, **F5**, and **F8**), or *para* (**N3**, **N6**, **N9**, **F3**, **F6**, and **F9**) to each other relative to the central arene. In addition, 1,4-bis(phenylethynyl)benzene (bisPEB) was examined as the parent molecule. For **N1–9**, the

(3) Samori, S.; Tojo, S.; Fujitsuka, M.; Splitler, E. L.; Haley, M. M.; Majima, T. *J. Org. Chem.* **2007**, *72*, 2785–2793.

(4) (a) Samori, S.; Hara, M.; Tojo, S.; Fujitsuka, M.; Yang, S.-W.; Elangovan, A.; Ho, T.-I.; Majima, T. *J. Phys. Chem. B* **2005**, *109*, 11735. (b) Samori, S.; Tojo, S.; Fujitsuka, M.; Yang, S.-W.; Elangovan, A.; Ho, T.-I.; Majima, T. *J. Org. Chem.* **2005**, *70*, 6661. (c) Samori, S.; Tojo, S.; Fujitsuka, M.; Yang, S.-W.; Ho, T.-I.; Yang, J.-S.; Majima, T. *J. Phys. Chem. B* **2006**, *110*, 13296. (d) Samori, S.; Tojo, S.; Fujitsuka, M.; Liang, H.-J.; Ho, T.-I.; Yang, J.-S.; Yang, S.-W.; Majima, T. *J. Org. Chem.* **2006**, *71*, 8732. (e) Samori, S.; Tojo, S.; Fujitsuka, M.; Lin, J.-H.; Ho, T.-I.; Yang, J.-S.; Majima, T. *J. Chin. Chem. Soc.* **2006**, *53*, 1225.

(5) (a) Goes, M.; Verhoeven, J. W.; Hofstraat, H.; Brunner, K. *ChemPhysChem* **2003**, *4*, 349. (b) Thomas, K. R. J.; Lin, J. T.; Tao, Y.-T.; Chuen, C.-H. *Chem. Mater.* **2002**, *14*, 3852. (c) Zhu, W.; Hu, M.; Yao, R.; Tian, H. *J. Photochem. Photobiol., A* **2003**, *154*, 169. (d) Thomas, K. R. J.; Lin, J. T.; Velusamy, M.; Tao, Y.-T.; Chuen, C.-H. *Adv. Funct. Mater.* **2004**, *14*, 83. (e) Chiang, C.-L.; Wu, M.-F.; Dai, D.-C.; Wen, Y.-S.; Wang, J.-K.; Chen, C.-T. *Adv. Funct. Mater.* **2005**, *15*, 231.

(6) (a) Elangovan, A.; Chen, T.-Y.; Chen, C.-Y.; Ho, T.-I. *Chem. Commun.* **2003**, 2146. (b) Elangovan, A.; Yang, S.-W.; Lin, J.-H.; Kao, K.-M.; Ho, T.-I. *Org. Biomol. Chem.* **2004**, *2*, 1597. (c) Elangovan, A.; Chiu, H.-H.; Yang, S.-W.; Ho, T.-I. *Org. Biomol. Chem.* **2004**, *2*, 3113. (d) Elangovan, A.; Kao, K.-M.; Yang, S.-W.; Chen, Y.-L.; Ho, T.-I.; Su, Y. O. *J. Org. Chem.* **2005**, *70*, 4460. (e) Yang, S.-W.; Elangovan, A.; Hwang, K.-C.; Ho, T.-I. *J. Phys. Chem. B* **2005**, *109*, 16628. (f) Lin, J.-H.; Elangovan, A.; Ho, T.-I. *J. Org. Chem.* **2005**, *70*, 7397.

(7) (a) Jayakannan, M.; Van Hal, P. A.; Janssen, R. A. J. *J. Polym. Sci., Part A Polym. Chem.* **2001**, *40*, 251. (b) Tykwinski, R. R.; Schreiber, M.; Carlon, R. P.; Diederich, F.; Gramlich, V. *Helv. Chim. Acta* **1996**, *79*, 2249. (c) Tykwinski, R. R.; Schreiber, M.; Gramlich, V.; Seiler, P.; Diederich, F. *Adv. Mater.* **1996**, *8*, 226. (d) Wilson, J. N.; Hardcastle, K. I.; Josowicz, M.; Bunz, U. H. F. *Tetrahedron* **2004**, *60*, 7157. (e) Wilson, J. N.; Smith, M. D.; Enkelmann, V.; Bunz, U. H. F. *Chem. Commun.* **2004**, 1700. (f) Wilson, J. N.; Josowicz, M.; Wang, Y.; Bunz, U. H. F. *Chem. Commun.* **2003**, 2962. (g) Miteva, T.; Palmer, L.; Kloppenburg, L.; Neher, D.; Bunz, U. H. F. *Macromolecules* **2000**, *33*, 652. (h) Zucchero, J. A.; Wilson, J. N.; Bunz, U. H. F. *J. Am. Chem. Soc.* **2006**, *128*, 11872. (i) Ojima, J.; Kakumi, H.; Kitatani, K.; Wada, K.; Ejiri, E.; Nakada, T. *Can. J. Chem.* **1984**, *63*, 2885. (j) Ojima, J.; Enkaku, M.; Uwai, C. *Bull. Chem. Soc. Jpn.* **1977**, *50*, 933.

(8) (a) Miller, J. J.; Marsden, J. A.; Haley, M. M. *Synlett* **2004**, 165. (b) Marsden, J. A.; Miller, J. J.; Shirtcliff, L. D.; Haley, M. M. *J. Am. Chem. Soc.* **2005**, *127*, 2464. (c) Spitler, E. L.; Shirtcliff, L. D.; Haley, M. M. *J. Org. Chem.* **2007**, *72*, 86. (d) Spitler, E. L.; Monson, J. M.; Haley, M. M *J. Org. Chem.* **2008**, *73*, 2211.

(9) (a) Marsden, J. A.; Palmer, G. J.; Haley, M. M. *Eur. J. Org. Chem.* **2003**, 2355. (b) Jones, C. S.; O'Connor, M. J.; Haley, M. M. In *Acetylene Chemistry: Chemistry, Biology, and Materials Science*; Diederich, F., Tykwinski, R. R., Stang, P. J., Eds.; Wiley-VCH: Weinheim, Germany, 2004; pp 303−385. (c) Marsden, J. A.; Haley, M. M. *J. Org. Chem.* **2005**, *70*, 10213. (d) Anand, S.; Varnavski, O.; Marsden, J. A.; Haley, M. M.; Schlegel, H. B.; Goodson, T., III. *J. Phys. Chem. A* **2006**, *110*, 1305. (e) Bhaskar, A.; Guda, R.; Haley, M. M.; Goodson, T., III. *J. Am. Chem. Soc.* **2006**, *128*, 13972. (f) Slepkov, A. D.; Hegmann, F. A.; Tykwinski, R. R.; Kamada, K.; Ohta, K.; Marsden, J. A.; Spitler, E. L.; Miller, J. J.; Haley, M. M. *Opt. Lett.* **2006**, *31*, 3315. (g) Spitler, E. L.; McClintock, S. P.; Haley, M. M. *J. Org. Chem.* **2007**, *72*, 6692.

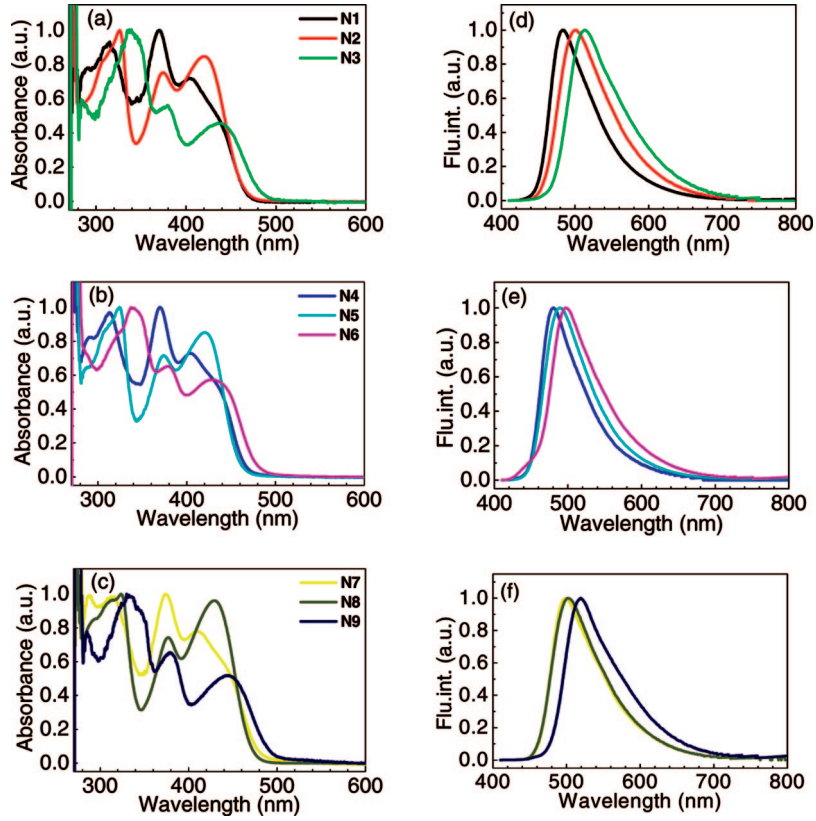

FIGURE 2. Absorption (a−c) and emission (d−f) spectra observed by the steady-state measurement of **N1–9** in Ar-saturated Bz. All solutions were prepared at a dilute concentration (10^{-5} M).

TABLE 1. Steady-State Spectral Properties of N1–9 in Ar-Saturated Bz

TAEB	λ_{max}^{Abs} (nm)	λ_{max}^{Fl} (nm)	E_{SI} (eV)[a]	Φ_{fl}	τ_{fl} (ns)
N1	(315), 370, (403), (451)	483	2.57	0.55	3.3
N2	326, (374), (421)	502	2.47	0.53	3.7
N3	337, (379), (439)	514	2.41	0.49	4.4
N4	(313), 370, (404)	480	2.58	0.54	3.3
N5	324, (374), (421)	489	2.54	0.53	3.2
N6	337, (378), (430)	496	2.50	0.45	3.6
N7	(313), 374, (410)	499	2.48	0.50	3.8
N8	323, (377), (429)	502	2.47	0.51	3.8
N9	330, (379), (444)	519	2.39	0.46	5.0

[a] Estimated from the peak wavelength of the fluorescence spectra (10^{-5} M).

TABLE 2. Steady-State Spectral Properties of F1–9 in Ar-Saturated Bz

TAEB	λ_{max}^{Abs} (nm)	λ_{max}^{Fl} (nm)	E_{SI} (eV)[a]	Φ_{fl}	τ_{fl} (ns)
F1	327, (376), (424)	490	2.53	0.44	3.4
F2	327, (376), (425)	493	2.52	0.54	3.4
F3	341, (381), (437)	506	2.45	0.48	4.1
F4	312, (380), (417)	506	2.45	0.41	4.0
F5	311, (384), (438)	514	2.41	0.47	4.4
F6	(338), 351, (384), (453)	531	2.34	0.40	5.7
F7	320, (380), (418)	505	2.46	0.30	3.9
F8	326, (381), 440	512	2.42	0.45	3.9
F9	330, (349), (384), (458)	534	2.32	0.40	5.0

[a] Estimated from the peak wavelength of the fluorescence spectra (10^{-5} M).

range of possible compounds expands greatly with variation of not only the substitution pattern of the donor or accepting unit but also the position of the nitrogen atom within the pyridine ring relative to the acetylenic linker (three possible positions). For **F1–9**, we can evaluate the cumulative effect of the number of acceptors per arene ring (three replacement types). The detailed study of 18 different kinds of donor-/acceptor-substituted TAEBs potentially leads to customization of optical band gaps for specialized material applications.

Results and Discussion

Steady-State Spectral Properties of TAEBs. Normalized steady-state absorption and fluorescence spectra of **N1–9** and **F1–9** in Bz are shown in Figures 2 and S1 (Supporting Information), respectively. All TAEBs showed a characteristic pattern with absorption bands as shown in Figure 2(a−c) and S1(a−c). It seems that the electronic structures of donor-/acceptor-substituted TAEBs strongly depend on the substitution pattern of the donor and/or acceptor groups because regioisomers (*ortho*-, *meta*-, and *para*-substituted isomers) have similar spectral shapes. Compared to neutral TPEB and tetra-donor TPEB, it was found that the corresponding absorption bands of the donor-/acceptor-substituted TAEBs are remarkably broadened and show further bathochromic shifts, indicating the intramolecular charge transfer (ICT) from the donor to the acceptor for the HOMO–LUMO transition.[8] TAEBs **N1–2**, **N4–5**, and **N7–8**, which possess linear-conjugated pathways, have a much more distinct low-energy band. Lacking the linear charge-transfer linkage, the low-energy bands of TAEBs **N3**, **N6**, and **N9** are weakened. This further indicates that the linear-conjugated pathways are more efficient than the "bent" conjugated or cross-conjugated donor to acceptor pathways.[8] The same spectral features were observed for the absorption spectra of **F1–9**.

Fluorescence was observed for **N1–9** and **F1–9** (Figure 2(d−f) and S1(d−f)). Compared to neutral TPEB or tetra-donor

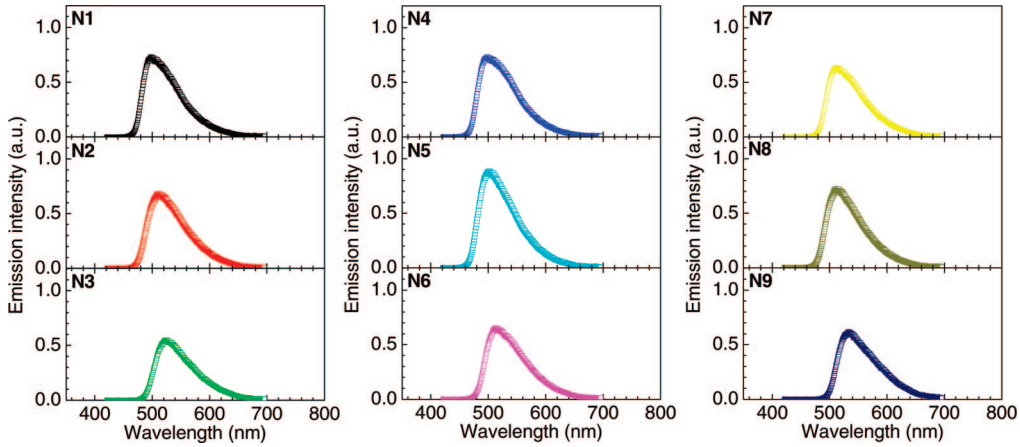

FIGURE 3. Emission spectra observed in the time range of 0–100 ns during the pulse radiolysis of **N1–9** in Ar-saturated Bz (0.5 mM).

SCHEME 3. Proposed Mechanism of the Emission During the Pulse Radiolysis of TAEBs in Bz[a]

$$Bz \rightsquigarrow e^- + Bz^{\bullet+}$$

$$Bz^{\bullet+} + e^- \rightarrow Bz^*$$

$$Bz^{\bullet+} + TAEB \rightarrow TAEB^{\bullet+}$$

$$e^- + TAEB \rightarrow TAEB^{\bullet-}$$

$$TAEB^{\bullet+} + TAEB^{\bullet-} \rightarrow {}^1TAEB^* + TAEB \text{ and } {}^3TAEB^* + TAEB \text{ (within pulse duration (8 ns))}$$

$$^1TAEB^* \rightarrow TAEB + h\nu_{fl}\ (\tau_{fl} < 8\ ns)$$

[a] For donor-/acceptor-substituted TAEBs (**N1–9** and **F1–9**), $^1TAEB^* = {}^1(A^{\bullet-}-D^{\bullet+})^*$ (ICT state).

TABLE 3. Emission Maxima (λ_{max}^{Em}) and Relative and Corrected Emission Intensities (*I*) during Pulse Radiolysis of N1–9 and bisPEB in Ar-Saturated Bz (0.5 mM)

compounds	λ_{max}^{Em} (nm)	I^a (%)
bisPEB	374	100
N1	498	31.9
N2	512	30.0
N3	522	22.8
N4	493	33.4
N5	502	38.8
N6	511	28.6
N7	511	26.8
N8	511	30.1
N9	533	24.8

[a] *I* values of TAEBs were determined from the integrated peak area based on the emission spectra observed during pulse radiolysis. Relative to *I* value of bisPEB in Ar-saturated Bz.

TPEB, donor-/acceptor-substituted TAEBs showed a large red-shift in the emission maxima in Bz. This again indicates ICT character for donor-/acceptor-substituted TAEBs in the S_1 state (Tables 1 and 2). Compared to *ortho* isomers, a slight red-shift of the fluorescence peak was observed for the corresponding *meta* isomers for **N1–9** and **F1–9**, indicating a bent-conjugated pathway (path c) leads to emission bands of longer wavelength than the cross-conjugated pathway (path b). In addition, compared to *ortho* or *meta* isomers, a slight red-shift of the fluorescence peak was observed for the corresponding *para* isomers, indicating TAEBs with both cross- (path b) and bent-conjugated (path c) pathways (or with no linear-conjugated pathways) lead to fluorescence bands of longer wavelength. It is also found that the fluorescence quantum yield (Φ_{fl}) values of **N1–9** ranged from 0.45 to 0.55 and showed the tendency for *ortho* (0.50–0.55), *meta* (0.51–0.53), and *para* isomers (0.49–0.45), in decreasing order. On the other hand,

TABLE 4. Emission Maxima (λ_{max}^{Em}) and Relative and Corrected Emission Intensities (*I*) during the Pulse Radiolysis of F1–9 and bisPEB in Ar-Saturated Bz (0.5 mM)

compounds	λ_{max}^{Em} (nm)	I^a (%)
F1	508	34.9
F2	508	34.6
F3	516	41.6
F4	522	12.7
F5	527	23.6
F6	541	25.7
F7	522	14.2
F8	522	21.7
F9	545	32.0

[a] *I* values of TAEBs were determined from the integrated peak area based on the emission spectra observed during pulse radiolysis. Relative to *I* value of bisPEB in Ar-saturated Bz.

TABLE 5. Electrochemical Properties of TAEBs and bisPEB in CH_3CN and Annihilation Enthalpy Changes ($-\Delta H°$), E_{S1}, and ($-\Delta H° - E_{S1}$) of TAEBs and bisPEB in Bz

	in CH_3CN		in Bz		
compounds	E_{ox} (V)	E_{red} (V)	$-\Delta H°$ (eV)	E_{S1} (eV)	$-\Delta H° - E_{S1}$ (eV)
N1	0.62	−1.89	2.70	2.57	+0.13
N2	0.62	−1.92	2.73	2.47	+0.26
N3	0.52	−1.87	2.58	2.41	+0.17
N4	0.54	−1.94	2.67	2.58	+0.09
N5	0.53	−1.99	2.71	2.54	+0.17
N6	0.53	−1.96	2.68	2.50	+0.18
N7	0.54	−1.85	2.58	2.48	+0.10
N8	0.55	−1.87	2.61	2.47	+0.14
N9	0.56	−1.82	2.57	2.39	+0.18
F1	0.56	−1.84	2.59	2.53	+0.06
F2	0.57	−1.87	2.63	2.52	+0.11
F3	0.55	−1.82	2.56	2.45	+0.11
F4	0.55	−1.75	2.49	2.45	+0.04
F5	0.55	−1.79	2.53	2.41	+0.12
F6	0.56	−1.74	2.49	2.34	+0.15
F7	0.62	−1.66	2.47	2.46	+0.01
F8	0.62	−1.70	2.51	2.42	+0.09
F9	0.65	−1.58	2.42	2.32	+0.10
bisPEB	1.38[a]	−2.35[a]	3.92	3.30	+0.62

[a] Ref 12.

Φ_{fl} values of **F1–9** ranged from 0.30 to 0.54 and showed the tendency for *meta* (0.45–0.54), *para* (0.40–0.48), and *ortho*-isomers (0.30–0.44), in decreasing order. For **N1–9**, low Φ_{fl} values of *para* isomers (**N3**, **N6**, and **N9**) can be explained by the energy-gap law.[10] From the peak positions of the

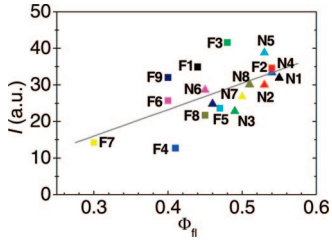

FIGURE 4. Plots of I value vs Φ_{fl} for TAEBs in Bz.

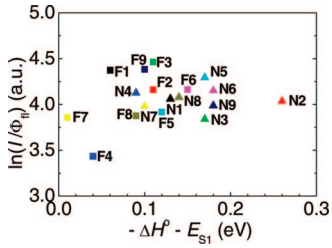

FIGURE 5. Plots of the $\ln(I/\Phi_{fl})$ vs $(-\Delta H^\circ - E_{S1})$ for TAEBs in Bz.

fluorescence spectra of **N3**, **N6**, and **N9**, the excitation energies of ^{1}**N3***, ^{1}**N6***, and ^{1}**N9*** (E_{S1} = 2.41, 2.50, and 2.39 eV, respectively) are estimated to be smaller than those of other ^{1}TAEBs* (2.47–2.58 eV). By laser flash photolysis of TAEBs in Bz, the quantum yields of the intersystem crossing (Φ_{ISC}) for **N1–9** and **F1–9** were found to be negligible ($\Phi_{ISC} < 0.1$). Thus, the internal conversion rates of **N3**, **N6**, and **N9** are faster than those of other TAEBs. In other words, the increase of internal conversion rate is responsible for the low Φ_{fl} values of *para* isomers. For **F1–9**, however, low values of *ortho* isomers cannot be explained by the energy-gap law because the excitation energies of ^{1}**F1***, ^{1}**F4***, and ^{1}**F7*** (E_{S1} = 2.53, 2.45, and 2.46 eV, respectively) are estimated to be larger than those of other ^{1}TAEBs* (2.32–2.52 eV). The details of the photophysical properties of **F1–9** are still unclear.

From the steady-state measurement, the emission color and intensity of donor-/acceptor-substituted TAEBs were found to be easily fine-tuned through control of the structural elements of the molecules. Obvious differences in fluorescence peaks and Φ_{fl} values were observed depending on the substitution pattern of the donor and/or acceptor groups, the position of the nitrogen atom within the pyridine ring, and the number of acceptors per arene ring.

Emission Generated from Charge Recombination between TAEB$^{\cdot+}$ and TAEB$^{\cdot-}$. Emission spectra were observed after an electron pulse during the pulse radiolysis of TAEBs in Ar-saturated Bz (0.5 mM) (Figures 3 and S2). According to previous reports,[3,4] the emission of TAEB indicates generation of ^{1}TAEB* by charge recombination of TAEB$^{\cdot+}$ and TAEB$^{\cdot-}$ generated during pulse radiolysis in Bz through the following plausible mechanism (Scheme 3). The same emission mechanism was assumed for bisPEB.

Little or no emission was observed during the pulse radiolysis of TAEBs in 1,2-dichloroethane (DCE) or *N*,*N*-dimethylformamide (DMF), indicating that TAEB$^{\cdot+}$ and TAEB$^{\cdot-}$ do not emit light. In other words, both TAEB$^{\cdot+}$ and TAEB$^{\cdot-}$ must be formed at the same time to emit light. In Bz, no transient absorption band of TAEB$^{\cdot+}$ and TAEB$^{\cdot-}$ was observed immediately after an 8 ns electron pulse. Therefore, it is assumed that TAEB$^{\cdot+}$ and TAEB$^{\cdot-}$ immediately recombine to give ^{1}TAEB* and ^{3}TAEB*, and ^{1}TAEB* emits light within a pulse duration. The transient absorption spectra observed during the pulse radiolysis of TAEBs in Ar-saturated Bz can be assigned to ^{3}TAEB*. Since the time profile of each ^{3}TAEB* decayed with second-order kinetics, it is assumed that ^{3}TAEB* mainly deactivates via triplet–triplet annihilation with no delayed fluorescence.[3,4]

Because of the considerable repulsion between the substituents induced by the rotation around C−C single bonds, a π-stacked structure cannot be formed for the interaction between TAEB$^{\cdot+}$ and TAEB$^{\cdot-}$. Therefore, TAEBs showed only monomer emission, although some electrochemiluminescent molecules showed both monomer and excimer emissions with less luminescence intensity during pulse radiolysis as mentioned in previous reports.[3]

N1–9 and **F1–9** showed emission peaks at 493–533 and 508–545 nm, respectively, and bisPEB did at 376 nm during the pulse radiolysis (Figures 3 and S2). The shape of the emission spectra of TAEBs was similar to those observed in the steady-state measurements, although the emission spectra of TAEBs were observed at the slightly longer wavelength due to the self-absorption as a result of the high concentrations.[3] Therefore, the formation of ^{1}TAEB* with ICT character can be assumed during pulse radiolysis. The intensity (I) of the radiolysis induced emission spectra of **N1–9**, **F1–9**, and bisPEB was determined from the integrated peak area based on the emission spectra observed during pulse radiolysis and summarized in Tables 3 and 4.

To elucidate the emission mechanism of TAEBs, we estimated the annihilation enthalpy change ($-\Delta H^\circ$) value for the charge recombination between M$^{\cdot+}$ and M$^{\cdot-}$. This $-\Delta H^\circ$ value is a criterion for whether ^{1}M* can be formed by the charge recombination or not.[2] $-\Delta H^\circ$ is calculated by eq 1[11]

$$-\Delta H^\circ = [(E_{ox} - E_{red})]^{\epsilon}{}_s - \Delta G_{sol}{}^{\epsilon}{}_s - w_{a,\mu} + T\Delta S^\circ \quad (1)$$

where E_{ox} and E_{red} are the oxidation and reduction potentials of M, respectively. ϵ_s, ΔG_{sol}, and $w_{a,\mu}$ represent the static dielectric constant of solvent, the free energy change of solvation, and the work required to bring M$^{\cdot+}$ and M$^{\cdot-}$ within a likely separation distance, respectively. For TAEBs and bisPEB in Bz, $-\Delta H^\circ$ can be expressed using E_{ox} and E_{red} measured in CH_3CN by simplified eq 2[3]

$$-\Delta H^\circ = E_{ox} - E_{red} + 0.19\ \text{eV} \quad (2)$$

The calculated $-\Delta H^\circ$ values for TAEBs and bisPEB are listed in Table 5, together with their oxidation and reduction potentials and E_{S1} values. $-\Delta H^\circ$ values for all TAEBs and bisPEB (2.42–3.92 eV) are consistently larger than their E_{S1} values (2.32–3.30 eV), indicating that the energy available in the charge recombination is sufficient to populate all TAEBs and bisPEB in the S_1 states.

As shown in Figure 4, the I value seems proportional to Φ_{fl}. However, the I value of some TAEBs deviates from the fitted line. In our previous paper,[4e] the energy differences between $-\Delta H^\circ$ and E_{S1} ($-\Delta H^\circ - E_{S1}$ (= 0.23–0.75 eV)) were assumed as one of the key factors for the I value of donor–acceptor type

(10) Kasha, M. *Chem. Rev.* **1947**, *41*, 401–419.
(11) Gross, E. M.; Anderson, J. D.; Slaterbeck, A. F.; Thayumanavan, S.; Barlow, S.; Zhang, S. R.; Marder, H. K.; Hall, M. F.; Nabor, J.-F.; Wang, E. A.; Mash, N. R.; Armstrong, R. M.; Wightman, Y. *J. Am. Chem. Soc.* **2000**, *122*, 4972.
(12) Kilsa, K.; Kajanus, J.; Macpherson, A. N.; Martensson, J.; Albinsson, B. *J. Am. Chem. Soc.* **2001**, *123*, 3069.

SCHEME 4. Proposed Structure for the Formation of TAEBs in the S_1 and T_1 States during Pulse Radiolysis in Bz

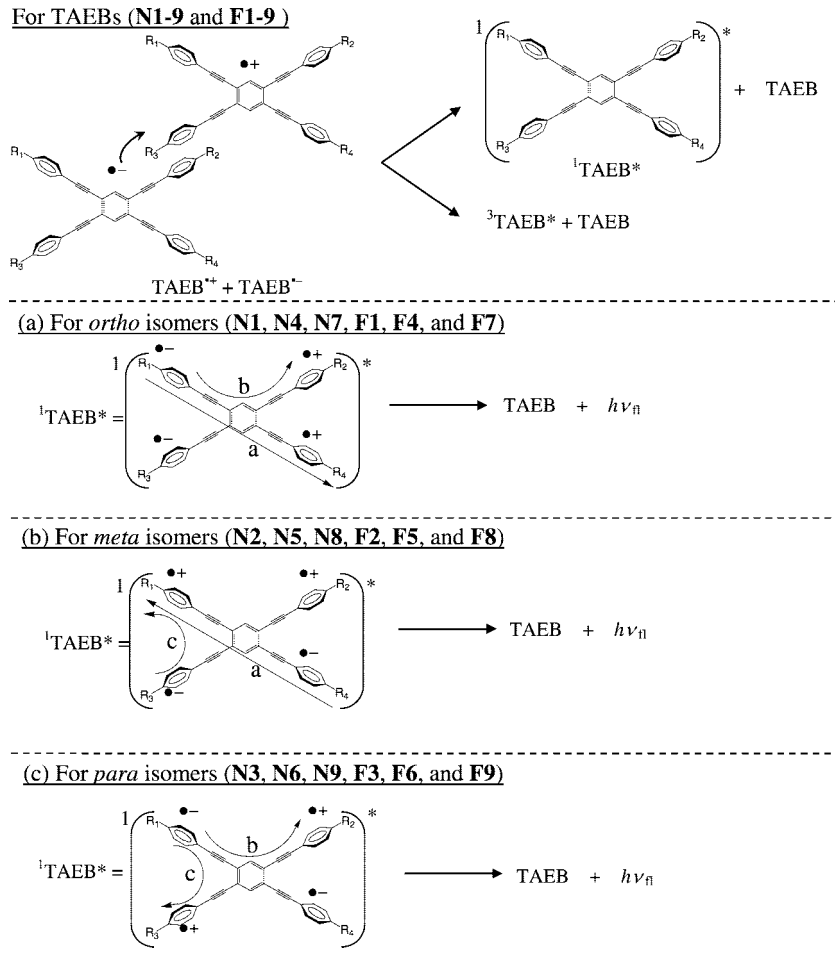

compounds. These deviated plots are assumed to be the range of errors or depend on not only Φ_{fl} but also the $(-\Delta H^\circ - E_{S1})$ value (Figure 5).[4e] However, no trend was observed in Figure 5. This might be due to the small $(-\Delta H^\circ - E_{S1})$ values of **N1–9** and **F1–9** (0.04–0.26 eV), indicating no clear effect of $(-\Delta H^\circ - E_{S1})$ on I value. However, it should be noted that the I values of **F4** and **F7** were lower than those of other TAEB. This behavior can be explained by their smaller Φ_{fl} (0.41 and 030, respectively) and $(-\Delta H^\circ - E_{S1})$ values (+0.04 and +0.01, respectively) among TAEBs.

Fine-Tuning of the Emission Color by Changing the Substitution Pattern of Donor-/Acceptor-Substituted TAEBs. Donor-/acceptor-substituted TAEBs can contain three types of conjugated pathways: linear-conjugated (path a), cross-conjugated

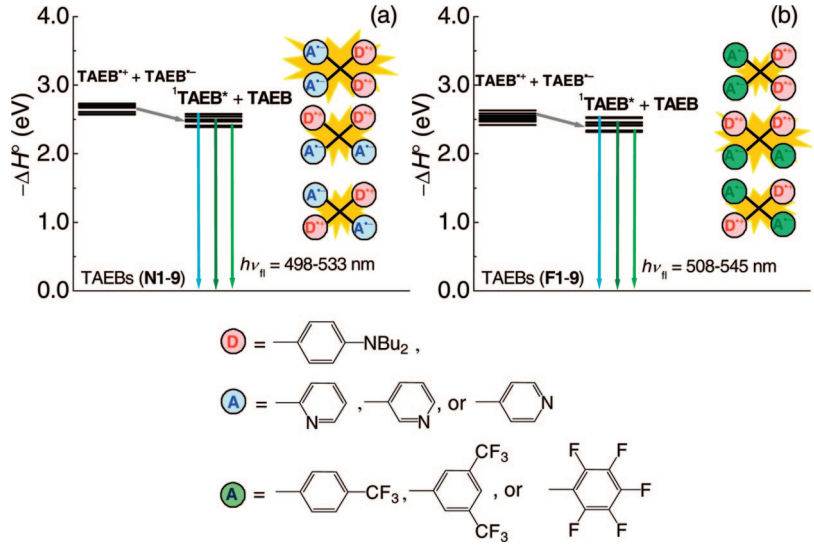

FIGURE 6. Energy level diagram for radiolysis induced chemiluminescence of **N1–9** (a) and **F1–9** (b). **D** and **A** denote electron donor- and electron acceptor-type molecules, respectively. $\mathbf{D}^{\bullet+}$ and $\mathbf{A}^{\bullet-}$ denote **D** radical cation and **A** radical anion, respectively.

(path b), and bent-conjugated (path c) pathways, as shown in Figure 1. The emission spectra of ^{1}TAEBs* with ICT character depends on the substitution pattern, the position of the nitrogen atom within the pyridine ring, and the number of acceptors per arene ring by the steady-state measurement and during the pulse radiolysis. The radiolysis induced emission spectra of all TAEBs showed emission bands in the region of wavelength where the fluorescence bands were observed by the steady-state measurements. Therefore, for *ortho*-(**N1**, **N4**, **N7**, **F1**, **F4**, and **F7**), *meta*-(**N2**, **N5**, **N8**, **F2**, **F5**, and **F8**), and *para*-substituted isomers (**N3**, **N6**, **N9**, **F3**, **F6**, and **F9**), it is suggested that the charge recombination between TAEB$^{\bullet+}$ and TAEB$^{\bullet-}$ generates ^{1}TAEB* with ICT character as shown in Scheme 4(a), 4(b), and 4(c), respectively.

Energy level diagrams for the radiolysis induced emission of TAEBs are shown in Figure 6. It is evident that judicious choice of the donor/acceptor unit permits control of the HOMO–LUMO energy gap, and thus the emission wavelengths can be fine-tuned at around 450–650 nm in the visible region.

Conclusions

Through control of the substitution pattern, the position of the nitrogen atom within the pyridine ring, or the number of acceptors per arene ring of the regioisomeric donor-/acceptor-substituted TAEBs **N1–9** and **F1–9**, fine-tuning of radiolysis induced emission color and intensity can be achieved. Using the pulse radiolysis technique, charge recombination between TAEB$^{\bullet+}$ and TAEB$^{\bullet-}$ gives ^{1}TAEB* as the emissive species, which has the emission peaks range 498–545 nm in the visible region. These specific emission properties of donor-/acceptor-substituted TAEBs may lead to customization of optical band gaps for specialized materials applications.

Experimental Section

Materials. 1,4-Bis(phenylethynyl)benzene (bisPEB) was purchased and purified by recrystallization from ethanol before use. TAEBs **N1–9** and **F1–9** were prepared according to the procedure previously described in the literature.[8c,d]

Measurements of Steady-State Spectral Properties. UV spectra were recorded in Bz with a UV/visible spectrometer using a transparent rectangular cell made from quartz (1.0 × 1.0 × 4.0 cm, path length of 1.0 cm). Fluorescence spectra were measured by a spectrofluorometer. The fluorescence quantum yields (Φ_{fl}) were determined by using coumarin 334 ($\Phi_{fl} = 0.69$ in methanol, $\lambda_{ex} =$ 400 nm)[13] standards.

Pulse Radiolysis. Pulse radiolysis experiments were performed using an electron pulse (28 MeV, 8 ns, 0.87 kGy per pulse) from a linear accelerator at Osaka University. All the sample solutions were prepared in a 0.5–10 mM concentration in Bz, 1,2-dichloroethane (DCE), or *N*,*N*-dimethylformamide (DMF) in a rectangular quartz cell (0.5 × 1.0 × 4.0 cm, path length of 1.0 cm). These solutions were saturated with Ar gas by bubbling for 10 min at room temperature before irradiation. The kinetic measurements were performed using a nanosecond photoreaction analyzer system. The monitor light was obtained from a pulsed 450 W Xe arc lamp, which was operated by a large current pulsed-power supply that was synchronized with the electron pulse. The monitor light was passed through an iris with a diameter of 0.2 cm and sent into the sample solution at a perpendicular intersection to the electron pulse. The monitoring light passing through the sample was focused on the entrance slit of a monochromator and detected with a photomultiplier tube. The transient absorption and emission spectra were measured using a photodiode array with a gated image intensifier as a detector. All emission spectra were corrected for the spectral sensitivity of the apparatus. The intensity (I) of the radiolysis induced emission spectra of **N1–9**, **F1–9**, and bisPEB was determined from the integrated peak area based on the emission spectra observed during pulse radiolysis. To avoid pyrolysis of the sample solution by the monitor light, a suitable cutoff filter was used.

Fluorescence Lifetime Measurements. Fluorescence lifetimes were measured by the single photon counting method using a streakscope equipped with a polychromator. Ultrashort laser pulses were generated with a Ti:sapphire laser (fwhm 100 fs) pumped with a diode-pumped solid-state laser. For the excitation of samples, the output of the Ti:sapphire laser was converted to the second (400 nm) with a harmonic generator.

Acknowledgment. We thank the members of the Radiation Laboratory of ISIR, Osaka Univ., for running the linear accelerator. This work has been partly supported by a Grant-in-Aid for Scientific Research (Project 17105005, 19350069, and others) from the Ministry of Education, Culture, Sports, Science and Technology (MEXT) of the Japanese Government and the US National Science Foundation (CHE-0414175). E.L.S. acknowledges the NSF for an IGERT fellowship (DGE-0549503). One of the authors (S.S.) expresses his thanks for a JSPS Research Fellowship for Young Scientists and the Global COE Program "Global Education and Research Center for Bio-Environmental Chemistry" of Osaka University.

Supporting Information Available: Absorption and emission spectra observed by the steady-state measurement of **F1–9** in Ar-saturated Bz (10^{-5} M). Emission spectra observed during the pulse radiolysis of **F1–9** in Ar-saturated Bz (0.5 mM). This material is available free of charge via the Internet at http://pubs.acs.org.

JO8001535

(13) Reynolds, G. A.; Drexhage, K. H. *Opt. Commun.* **1975**, *13*, 222.